Accepted manuscript doi:
10.1680/jgele.18.00108

Submitted: 18 June 2018

Published online in 'accepted manuscript' format: 03 October 2018

Manuscript title: Hydraulic conductivity from CPTu on-the-fly: a numerical evaluation

Authors: L. Monforte[1], M. Arroyo[1], A. Gens[1] and J. M. Carbonell[2]

Affiliations: [1]Departamiento de Ingeniería del Terreno, UPC, Barcelona, Spain and [2]CIMNE, Barcelona, Spain

Corresponding author: Lluís Monforte, Departamiento de Ingeniería del Terreno, UPC, Barcelona, Spain and [2]CIMNE, Barcelona, Spain. Tel.: +34 618302232.

E-mail: lluis.monforte@upc.edu

Accepted manuscript doi:
10.1680/jgele.18.00108

Abstract

Permeability is important in many geotechnical applications. The current CPTu practice to obtain permeability values relies on dissipation tests, which are frequently slow and only linked to permeability through compressibility measures. On-the-fly methods offer an alternative approach in which permeability is directly linked to CPTu penetration measurements. Several on-the-fly methods have been proposed and their applicability and relative advantages are not fully clear. Numerical effective stress simulation of CPTu testing is used here to explore in a simplified but realistic setting the relative merits of different on-the-fly methods. It is found that for partly drained materials the original simpler relation between cone metrics and normalized permeability works reasonably well. A continuous generalization of Elsworth and Lee method to the full permeability range is proposed, noting the connection to the backbone normalized pore pressure curve that describes the partly drained transition of cone penetration. The importance of an undrained limit beyond which the method produces large errors is stressed.

Keywords: Permeability; in-situ testing; CPTu; numerical analysis; PFEM

Accepted manuscript doi:
10.1680/jgele.18.00108

1 Introduction

Hydraulic conductivity (or simply "permeability" in accepted geotechnical parlance) is one of the fundamental properties of soils with wide implications for geotechnical design. Evaluation of permeability in the laboratory is frequently complicated by scale-dependency, anisotropy and sample disturbance. Field tests might partly avoid these complications but generally require more involved interpretation procedures and –for pumping tests- larger investments.

The piezocone (CPTu) test is one of the more cost-effective site investigation tools, widely used for stratigraphic delineation, direct structural design and soil property evaluation. Current standard procedures (e.g. EN ISO 22476-1:2012) prescribe dissipation tests when drainage and/or consolidation characteristics are to be evaluated. In a dissipation test, the CPTu penetration is halted and the pore pressure decay in time is registered. The duration of a dissipation test is usually established as that required to achieve a 50% reduction of the pore pressure registered just before the stoppage. This time is denoted t_{50} and to attain it holding times of several hours are very frequently necessary.

Direct correlations between t_{50} and permeability, *k*, have been proposed (Parez & Fauriel, 1988; Mayne, 2007). Nevertheless, dissipation tests are most frequently interpreted by means of normalized dissipation curves proposed by Teh & Houlsby (1991). These link measured dissipation time to a consolidation coefficient, *c*. For instance, for measurements taken at the cone shoulder, a frequently used formula is

$$c = \frac{0.245\, r^2 \sqrt{I_r}}{t_{50}} = \frac{kM}{\gamma_w} \qquad (1)$$

Where *r* is the cone tip radius, γ_w is water unit weight, I_r is a rigidity index, and M is a constrained modulus. The rigidity index is defined as G/s_u, the ratio between a shear modulus *G* and an undrained shear strength s_u. Obtaining appropriate values for *G* and s_u is not always easy (Schnaid et al. 1997). When a value of permeability, *k*, is necessary, an estimate of constrained modulus, *M*, is also required, which compounds the difficulties.

Elsworth & Lee (2005, 2007) proposed an alternative method in which permeability could be directly estimated from the CPTu data stream without the need for any stoppage. This work was restricted to materials, like silts, in which CPTu penetration was partly drained. Later work (Chai et al. 2011; Shen et al. 2015) has sought to extend that approach to more impermeable materials. These methods are attractive, although some difficulties in application have been reported (Vessia et al. 2012). Direct experimental verification is complicated by the factors mentioned above. The purpose of this letter is to use an advanced numerical modelling technique to explore the performance of on-the-fly CPTu hydraulic conductivity measurement methods in an idealized setting.

Accepted manuscript doi:
10.1680/jgele.18.00108

2 On-the-fly evaluation of permeability using CPTu

2.1 Elsworth & Lee method

Elsworth and Lee (2005), generalizing previous work by Elsworth (1993), analyzed the flow induced by a finite size penetrometer as a moving steady state flow problem. Combining dislocation and cavity expansion analysis and assuming negligible local storage they used continuity and Darcy's law to obtain the following relation

$$\frac{\Delta u}{\sigma_{v0}^{'}} = \frac{v r \gamma_w}{4k\sigma_{v0}^{'}} = \frac{1}{K_D^E} \tag{2}$$

Where Δu is excess pore pressure at the cone, σ'_{v0} is the in situ vertical effective stress and v is the rate of cone advance. The symbol K_D^E represents a dimensionless ratio. Elsworth and Lee (2005) noted that the relation obtained could be expressed using only conventional normalized CPTu metrics as

$$K_D^E = \frac{1}{B_q Q_t} \tag{3}$$

Where the normalized pore pressure factor B_q and cone tip resistance Q_t are given by

$$\begin{aligned} B_q &= \frac{\Delta u}{q_t - \sigma_{v0}} \\ Q_t &= \frac{q_t - \sigma_{v0}}{\sigma'_{v0}} \end{aligned} \tag{4}$$

The formulation allows on-the-fly estimation of permeability from the CPTu record, without any stoppage. The analysis leading to equation (2) could not distinguish between different pore pressure measurement positions at the cone tip. For practical reasons, later development of the method has always been based on measurements just above the shoulder, at the so-called u_2 position (Figure 1). This is also assumed here, although for notational convenience we drop the subscript.

Equations (2) and (3) clearly imply that B_q does not only depend on OCR or soil state, as was traditionally assumed. Partial drainage may also affect that value: as a consequence a soil classification chart (Robertson, 1990) based on Q_t and Bq is unable to distinguish trends due to increasing OCR and to increased consolidation. Schneider et al. (2008) proposed a new classification chart that avoided this problem by using $\frac{\Delta u_2}{\sigma'_{v0}}$ instead of B_q.

Accepted manuscript doi:
10.1680/jgele.18.00108

2.2 Subsequent work

Elsworth & Lee method assumed no storage of water around the penetrating cone. This implies that the method is not applicable in highly dilatant materials. Experimental work by Chai & Chamee (2017) with overconsolidated clay has confirmed this limitation.

There is less consensus about the requirement of partial drainage. According to Elsworth & Lee (2007), the method should not be applied below a certain undrained limit. Using classical results from spherical cavity expansion analysis and setting Skempton pore pressure coefficient A = 1 they arrived at the following expression for the undrained limit

$$\left(B_q Q_t\right)_u = \frac{\Delta u_{ref}}{\sigma'_{v0}} = \frac{4}{3}\frac{s_u}{\sigma'_{v0}} \ln I_r \tag{5}$$

Where Δu_{ref} corresponds to the pore pressure developed under fully undrained conditions. For typical values of the rigidity index I_r and the undrained strength ratio $\frac{s_u}{\sigma'_{v0}}$, they argued that the limit value would vary between 1.2 and 5.6. Elsworth & Lee (2007) went on to analyze the performance of the method, comparing CPT_u results with K_D^E values derived from laboratory measurements. From this comparison a generalized form of the original proposal followed, which can be expressed as

$$K_D^E = \frac{\alpha}{\left(B_q Q_t\right)^{\beta}} \tag{6}$$

where α, β are empirical coefficients introduced to obtain a good fit with the supporting database. The values proposed (see Table 1) were α = 0.62 and β = 1.6.

Chai et al. (2011) revisited the method, introduced some modifications in the geometrical assumptions used to derive the basic formula, and examined its performance extending the original dataset. They rejected the idea of an undrained limit, arguing that even for highly impermeable materials some flow does take place. Although they used slightly different definitions, their proposal can be rearranged in the form of equation (6), using a piece-wise formulation with two different expressions having non-overlapping ranges of application (see Table 1).

Shen et al (2015) maintained the full range of application proposed by Chai et al. (2011). They reexamined again the geometrical assumptions of the derivation, to introduce a more realistic representation of the cone tip. They also introduced some soil-type influence on the assumed excess pore pressure moving steady-state distribution around the tip. All this resulted in a slightly modified formulation that, for the case of the standard cone tip angle (60°) may be again recast in the form of a piece-wise equation (6) with parameters that now depend somewhat on soil type (Table 1).

Accepted manuscript doi:
10.1680/jgele.18.00108

3 Numerical approach

3.1 G-PFEM

The numerical code G-PFEM (Geotechnical Particle Finite Element Method) has been specifically developed for the analysis of large strain contact problems in geomechanics (Monforte et al, 2017a, 2018a). PFEM (Oñate et al., 2004,2011) is a particle method supported by a mesh: the solution is computed in a finite element mesh built with well-shaped element simplexes. This computational mesh evolves during problem solution through frequent remeshing of a cloud of particles. A Lagrangian description of the continuum is used and the information between meshes is transferred using interpolation algorithms. This general PFEM scheme is enriched with the inclusion of rigid bodies of specified motion that may contact, penetrate and reshape the discretized continuum.

Low order finite elements are used in the G-PFEM, e.g. linear triangles in two-dimensional models. Interpolation is thus simplified and the computational cost reduced with respect to methods using higher-order elements. In order to avoid locking stabilized mixed formulations are required (Monforte et al, 2017b).

The constitutive equations in G-PFEM are formulated in a large strain framework. Integration is performed using an explicit scheme with substepping (Sloan et al. 2001), adapted to large strains (Monforte et al. 2015). G-PFEM is implemented into Kratos Multiphysics framework (Dadvand et al. 2010), an object-oriented multi-disciplinary open-access platform for numerical analysis tool development.

3.2 Simulation database

Results from two sets of simulations are presented below. The first one (set A in Table 2) was part of a larger parametric study of dissipation test responses using a frictionless cone (Parolini, 2016). The second set (set B in Table 2) was performed to study of the effect of side friction on the partly drained penetration response (Monforte et al. 2018a). The code was run in a fully-coupled mode, assuming quasi-static conditions (u-p_w formulation). In all simulations the cone has the standard dimensions (R = 1.78 cm; cone angle 60°) and is assumed rigid. It is initially wished-in-place with the tip at depth of z = 2R and is then advanced to a depth of z = 20R at the standard velocity (v = 0.02 m/s). The geometry of the problem is sketched in Figure 1; due to the geometry of the problem, an axisymmetric model is employed.

The material is described by a Modified Cam Clay constitutive model, with two tweaks that enhance numerical robustness. These refer to the elastic part (which follows a hyperelastic formulation, see Borja et al.1997) and to the deviatoric extension of the yield surface (reformulated to ensure convexity, see Panteghini & Lagioia, 2014). Soil parameters are listed in Table 2. In both cases they describe a quasi-normally consolidated clayey deposit, hence no plastic dilation is expected. Material A is more rigid and somewhat stronger.

Accepted manuscript doi:
10.1680/jgele.18.00108

In set A, the weight of the soil is considered and, at the boundary, a vertical stress of 100 kPa is prescribed; whereas in set B, the soil is assumed weightless and the initial vertical stress is 57.85 kPa. Inertial effects are neglected in both sets of simulations. In set A the cone is assumed frictionless, whereas in set B the cone interface strength is described by different values of the effective friction angle δ´ (Table 2).

4 Results

A clear steady state is identified in the simulations after about 5 radius penetration. Examples are shown in Figure 2 where the more compressible nature of set B is evidenced. As explained in Monforte et al (2018a) remeshing induces some numerical noise, particularly in simulations with high interface friction. The penetration curves (Figure 2) were then smoothed before interpretation, using a moving average of 0.3 R.

Bq values for the simulations are in the range 0 to 1 which is fairly common in the field. Indeed, when the numerical results are plotted in common interpretation charts (Figure 3) they fall where expected. In the Robertson (1990) chart they always lie in zone 3 and classify as "clays - clay to silty clay". In the Schneider et al (2008) graph they move from clays (zone 1b) to silts (zone 1a) and then to transitional soils (zone 3) as permeability increases. Similar observations were reported by other researchers using MCC to numerically simulate CPT (e.g. Ceccatto et al. 2016)

Figure 4 presents the pore pressure field normalized by the u_2 at z = 20R value for different permeabilities. As expected (Teh & Houlsby, 1991) the highest pore pressure is observed just ahead of the cone shoulder reaching approximately 1.5 times the u_2. An assumption of spherical symmetry for the pore pressure steady state disturbance is present in the derivations of equation (6). The numerical results show that the shape of the moving disturbance becomes somewhat more elongated as the permeability decreases (Figure 4). A similar effect was noted by Yi et al (2012) when varying penetration rate and keeping permeability constant. Examining in more detail that shape (Figure 5) it appears that the spherical symmetry assumption is more questionable when looking closer to the cone tip (direction given by γ = -90° in Figure 5) and that the asymmetry is more marked as permeability decreases.

Figure 6 compares the simulated results with Elsworth & Lee (2005) equation (3) and their more elaborate later proposal in Elsworth & Lee (2007). Despite its simplicity, equation (3) seems to offer a close limit for the more drained materials (with K_D^E > 0.33 corresponding here to *k* above $5 \cdot 10^{-6}$ m/s). Considering Elsworth & Lee (2007), the numerical results do not support the introduction of a value of β > 1 in equation (6); on the other hand, the undrained limit ($B_q Q_t$ = 1.2) offers a good indication of the limit beyond which a single equation (6) is valid.

Accepted manuscript doi:
10.1680/jgele.18.00108

Figure 7 compares the simulated results with the proposals of Chai et al (2011) and Shen et al (2015). These piecewise formulations improve somewhat the comparison with the numerical results in the intermediate K_D^E range, but are clearly offset at the more drained end and introduce large errors at the more impermeable end.

5 Discussion

A more versatile generalization of the original Elsworth equation may be obtained using a different angle. Partly drained CPTu penetration has received much attention because it may introduce substantial error in conventional CPTu interpretation methods (De Jong & Randolph, 2012). For given soil parameters and initial state, partly drained penetration results in increased tip resistance and decreased excess pore pressure (Randolph & Hope, 2004).

A backbone curve model was proposed by (De Jong & Randolph, 2012; De Jong et al. 2013) to express the change in CPTu induced excess pore pressure, Δu as a function of normalized penetration velocity, V

$$\frac{\Delta u}{\Delta u_{ref}} = 1 - \frac{1}{1+\left(\frac{V}{V_{50}}\right)^c} \tag{7}$$

Where Δu_{ref} is the value during fully undrained penetration and c and V_{50} are adjustment coefficients. The normalized penetration velocity is given by

$$V = 2\frac{vr}{c} = 2\frac{\lambda \gamma_w v r}{\sigma'_{v0} k \left(1+e_0\right)} \tag{8}$$

Where the coefficient of consolidation c, has been selected as that governing vertical consolidation at the “in situ” condition for a normally consolidated cam-clay material.

Making use of the previously defined normalized permeability, the excess pore pressure backbone curve can be expressed as

$$\frac{\Delta u}{\Delta u_{ref}} = 1 - \frac{1}{1+\left(\frac{8}{\left(1+e_0\right)V_{50}}\frac{\lambda}{K_D^E}\right)^c} \tag{9}$$

and, introducing the normalized metrics B_q and Q_t, it follows that

$$B_q Q_t = \frac{a\, d^c}{\left(K_D^E\right)^c + d^c} \tag{10}$$

Accepted manuscript doi:
10.1680/jgele.18.00108

Where two non-dimensional groupings denoted a, d are introduced to denote

$$a = \frac{\Delta u_{ref}}{\sigma'_{v0}}$$
$$d = \frac{8\lambda}{(1+e_0)V_{50}} \quad (11)$$

It is clear that expression (10) is quite similar to expression (6) and may be seen as a continuous generalization of the Elsworth & Lee (2007) original expression. This continuous generalization clearly incorporates the undrained limit as an asymptote (as $K_D^E \to 0$ then $B_q Q_t \to a$). This limiting role of a is made clearer by inverting expression (10) so that

$$K_D^E = d\left(\frac{a}{B_q Q_t} - 1\right)^{\frac{1}{c}} = d\left(\frac{\Delta u_{ref}}{\Delta u} - 1\right)^{\frac{1}{c}} \quad (12)$$

A explicit expression for permeability may be obtained combining (12), (11) and (2)

$$k = \frac{v\, d_c\, \gamma_w}{\sigma'_{v0}} \frac{\lambda}{(1+e_0)V_{50}} \left(\frac{\Delta u_{ref}}{\Delta u} - 1\right)^{\frac{1}{c}} \quad (13)$$

The number of adjustment parameters involved this continuous generalization is five, (c, V_{50}, Δu_{ref} or a , λ, e_0), a number identical to those in the piecewise generalizations. Two parameters (λ, e_0) may be independently measured. The undrained limit a may be approximated with expressions such as (5). Figure 8 presents a parametric analysis of expression (10). It is interesting to note that values of $\beta > 1$ suggested from field data by Elsworth & Lee (2007) would imply a steeper backbone curve (i.e. higher values of c).

De Jong & Randolph, (2012) suggested default values of c = 1 and V_{50} = 3. Figure 9 plots expression (10) using those default values, evaluating a = 1.9 with approximation (5) and using the plastic compressibility and void ratio input to series B. A good fit appears, in line with that obtained for the backbone expression (7) by Monforte et al (2018a).

The undrained limit value a (or equivalently Δu_{ref}) plays a prominent role when applying this method. Note, for instance, that all values of $B_q Q_t$ that plot above the asymptote a = 1.9 in Figure 9 cannot be used to estimate

permeability. For these numerical simulations more precise values of Δu_{ref} are readily available (giving a = 1.91 for series B but a = 2.47 for series A). Using those more precise values in Equation (13), the deduced permeability values are compared with the input permeability values in Figure 10. For values of permeability below 10^{-6} m/s the method appears too imprecise. A similar comparison using the previous proposals is presented in Figure 11, showing that their performance is not better.

6 Conclusion

For partially drained penetration CPTu the on–the-fly method appears to offer a good approximation to the evaluation of permeability in compressible soils. The continuous generalization proposed here offers a clear connection with studies on partially drained penetration and clarifies the meaning of the adjustment parameters. The method does not seem appropriate for the more undrained materials, ($k < 10^{-6}$ m/s) where dissipation is more onerous. Using similar analyses, Monforte et al (2018b) show that methods based on direct correlation with t_{50} work well for fully undrained conditions.

Field validation of the on-the-fly method is challenging because of factors such as permeability anisotropy, layering, sample disturbance and scale effects. Refinement of G-PFEM to incorporate some of those factors is currently under way (Hauser et al. 2018); it is then hoped that numerical simulation will continue to support further exploration and validation of this limited, but still potentially useful method.

Acknowledgements

This work has been supported by the Ministry of Science and Innovation of Spain through research grant BIA2017-84752-R.

Accepted manuscript doi:
10.1680/jgele.18.00108

List of notation

B_q	normalized pore pressure factor
c	consolidation coefficient
c, V_{50}	parameters of DeJong & Randolph backbone curve
$\boldsymbol{d}, d_r$	displacement, radial displacement
d_c	diameter of the cone
e_0	initial void ratio
G	shear modulus
I_r	rigidity index
K_0	coefficient of earth pressure
K_D^E	dimensionless permeability
k	permeability
M	constrained modulus
M	slope of the critical state line
Q_t	normalized cone tip resistance
r	radius of the cone
S_u	undrained shear strength
v	rate of cone advance
V	normalized penetration velocity
α, β	parameters of the on-the-fly interpretation method
Δu	excess water pressure at the u_2 position
δ'	interface friction angle
Δu_{ref}	excess water pressure at the u_2 position during fully undrained penetration
γ_w	water unit weight
Δu	excess water pressure at the u_2 position
κ	swelling slope
λ	slope of the virgin consolidation line
σ'_{vo}	in situ vertical effective stress

References

Borja RI, Tamagnini C, Amorosi A. (1997) Coupling plasticity and energy-conserving elasticity models for clays. J Geotech Geoenviron Eng;123(10):948–57.

Ceccato, F., Beuth, L., & Simonini, P. (2016). Analysis of piezocone penetration under different drainage conditions with the two-phase material point method. Journal of Geotechnical and Geoenvironmental Engineering, 142(12), 04016066.

Chai, J. and N. Chanmee (2017). A modified method for estimating the permeability of clayey soils based on piezocone sounding results. Canadian Geotechnical Journal (accepted)

Chai, J. C., P. M. A. Agung, T. Hino, Y. Igaya, and J. P. Carter (2011). Estimating hydraulic conductivity from piezocone soundings. Géotechnique 61 (8), 699–708.

Dadvand, P., R. Rossi, and E. Oñate (2010). An object-oriented environment for developing finite element codes for multi-disciplinary applications. Archives of computational methods in engineering 17 (3), 253–297.

DeJong, J. T. and M. F. Randolph (2012). Influence of partial consolidation during cone penetration on estimated soil behavior type and pore pressure dissipation measurements. Journal of Geotechnical and Geoenvironmental Engineering 138 (7), 777–788.

DeJong, J. T., Jaeger, R. A., Boulanger, R.W., Randolph, M.F. and Wahl, D.A.J (2013). Variable penetration rate cone testing for characterization of intermediate soils. In 4th International Site Characterization Conference, Volume 4, pp 25-42.

EN ISO 22476-1:2012, (2012). Geotechnical Investigation and Testing - Field Testing – Part 1: Electrical Cone and Piezocone Penetration Test

Elsworth, D. (1993). Analysis of piezocone dissipation data using dislocation methods. Journal of Geotechnical Engineering, 119(10), 1601-1623.

Elsworth, D. and D. S. Lee (2007). Limits in determining permeability from on-the-fly uCPT sounding. Géotechnique 57 (8), 679–685

Elsworth, D. and D. S. Lee (2005). Permeability determination from on-the-fly piezocone sounding. Journal of Geotechnical and GeoEnvironmental engineering 131 (5), 643–653.

Hauser, L., Schweiger, H.F., Monforte, L. & Arroyo, M. (2018) Numerical study of anisotropic permeability effects on undrained CPTu penetration, 4th International Symposium on Cone Penetration Testing, CPT'18

Mayne, P. W. (2007). Cone penetration testing (Vol. 368). Transportation Research Board.

Monforte, L., Arroyo, M., Carbonell, J. M., & Gens, A. (2018a). Coupled effective stress analysis of insertion problems in geotechnics with the particle finite element method. Computers and Geotechnics 101, 114–129, doi.org/10.1016/j.compgeo.2018.04.002

Monforte, L., Arroyo, M., Gens, A. & Parolini, C. (2018b) Permeability estimates from CPTu: a numerical study, 4th International Symposium on Cone Penetration Testing, CPT'18

Monforte, L., Arroyo, M., Carbonell, J. M., & Gens, A. (2017a). Numerical simulation of undrained insertion problems in geotechnical engineering with the Particle Finite Element Method (PFEM). Computers and Geotechnics, 82, 144-156. DOI:/10.1016/j.compgeo.2016.08.013

Monforte, L; Carbonell, J.M; Arroyo, M & Gens, A. (2017b) Performance of mixed formulations for the Particle Finite Element Method in soil mechanics problems, Computational Particle Mechanics, DOI 10.1007/s40571-016-0145-0

Monforte, L., M. Arroyo, A. Gens & J. M. Carbonell (2015). Explicit finite deformation stress integration of the elasto-plastic constitutive equations. In The 14th International Conference of the International Association for Computer Methods and Advances in Geomechanics (14IACMAG).

Oñate E, Idelsohn SR, Del Pin F, Aubry R. (2004) The particle finite element method—an overview. Int J Comput Methods1(02):267–307.

Oñate, E., S. R. Idelsohn, M. A. Celigueta, R. Rossi, J. Marti, J. M. Carbonell, P. Ryzakov, and B. Suárez (2011). Advances in the particle finite element method (PFEM) for solving coupled problems in engineering. In In Particle-Based Methods, pp. 1–34. Springer Netherlands.

Parez, L., & Fauriel, R. (1988). Le piézocône améliorations apportées à la reconnaissance des sols. Revue française de géotechnique, (44), 13-27.

Panteghini A, Lagioia R. (2014) A fully convex reformulation of the original Matsuoka- Nakai failure criterion and its implicit numerically efficient integration algorithm. Int J Numer Anal Meth Geomech;38:593–614. http://dx.doi.org/10.1002/nag.2228.

Parolini, C. (2016) CPT and dissipation test simulation through PFEM, MSc thesis, Politecnico di Milano

Randolph, M. F. and S. Hope (2004). Effect of cone velocity on cone resistance and excess pore pressures. In Int. Symp. on Engineering Practice and Performance of Soft Deposits, pp. 147–152.

Robertson, P. K. (1990). Soil classification using the cone penetration test. Canadian Geotechnical Journal 27 (1), 151–158.

Schnaid, F., Sills, G. C., Soares, J. M., & Nyirenda, Z. (1997). Predictions of the coefficient of consolidation from piezocone tests. Canadian Geotechnical Journal, 34(2), 315-327.

Schneider, J. A., M. F. Randolph, P. W. Mayne, and N. R. Ramsey (2008). Analysis of factors influencing soil classification using normalized piezocone tip resistance and pore pressure parameters. Journal of Geotechnical and Geoenvironmental Engineering 134 (11), 1569–1586

Shen, S. L., Wang, J. P., Wu, H. N., Xu, Y. S., Ye, G. L., & Yin, Z. Y. (2015). Evaluation of hydraulic conductivity for both marine and deltaic deposits based on piezocone testing. Ocean Engineering, 110, 174-182.

Sloan, S. W., A. J. Abbo, and D. Sheng (2001). Refined explicit integration of elastoplastic models with automatic error control. Engineering Computations 18 (1-2), 121–194.

Teh, C. I. and G. T. Houlsby (1991). An analytical study of the cone penetration test in clay. Géotechnique 41 (1), 17–34.

Vessia, G., Casini, F., & Springman, S. (2012). Discussion: estimating hydraulic conductivity from piezocone soundings. Géotechnique, 62, 955-956.

Yi, J. T., S. H. Goh, F. H. Lee, and M. F. Randolph (2012). A numerical study of cone penetration in fine-grained soils allowing for consolidation effects. Géotechnique 62 (8), 707–719.

Accepted manuscript doi:
10.1680/jgele.18.00108

Tables

Table 1 Proposed empirical fittings of the generalized Elsworth & Lee relation

Reference	**Range of application**	**α**	**β**
Elsworth & Lee (2007)	$B_qQ_t < 1.2$	0.62	1.6
Chai et al. (2011)	$B_qQ_t < 0.45$	2	1
Chai et al. (2011)	$0.45 < B_qQ_t$	0.088	4.91
Shen et al. (2015) (Clay)	$B_qQ_t < 0.45$	0.8 – 3.74	1
Shen et al. (2015) (Clay)	$0.45 < B_qQ_t$	0.035 – 0.16	4.91

Table 2 Material parameters employed in the G-PFEM simulations of CPTu

Simulation set	κ	λ	e_0	G (kPa)	α	ν	M	OCR	k (m/s)	δ' (°)	K_0
A Parolini (2016)	0.02	0.2	1.94	10000	0	0.18	1.07	1.1	10^{-7} – 10^{-12}	0	0.765
B Monforte et al. (2018a)	0.05	0.3	2.0	400	23.5	0.33	1	1.21	10^{-3} – 10^{-8}	0, 10, 20, 25	0.5

Accepted manuscript doi:
10.1680/jgele.18.00108

Figure captions

Figure 1 G-PFEM CPTu penetration example. Sketch of the geometrical and boundary conditions, (a), and mesh after 20 radii of penetration, (b).

Figure 2 Example penetration records from the simulations with $k = 10^{-8}$ m/s assuming a smooth interface.

Figure 3 Numerical results depicted in custom interpretation charts

Figure 4 Normalized water pressure contours at steady state (penetration 20 radii) for different permeability. Set B, smooth interface.

Figure 5 Effect of permeability on normalized pore pressure variations with normalized distance to the u_2 position along different directions

Figure 6 Comparison of simulated results with Elsworth & Lee proposals

Figure 7 Comparison of simulated results with piece-wise extensions of Elsworth & Lee proposals

Figure 8 Effect of different input parameters in the continuous generalized Elsworth expression In panel (c) $\lambda^* = \lambda/(1+e_0)$. The thick black lines represent Elsworth & Lee (2007)

Figure 9 Comparison of simulated results with Equation (10) with c = 1, V_{50} = 3, a = 1.9, λ = 0.3, e_0 = 2

Figure 10 Comparison of input permeability to the numerical calculations and that deduced from Equation (13) with c = 1, V_{50} = 3, and values of a, λ, e_0 appropriate for each series

Figure 11 Comparison of input permeability to the numerical calculations and that deduced from previous on-the-fly proposals

Accepted manuscript doi:
10.1680/jgele.18.00108

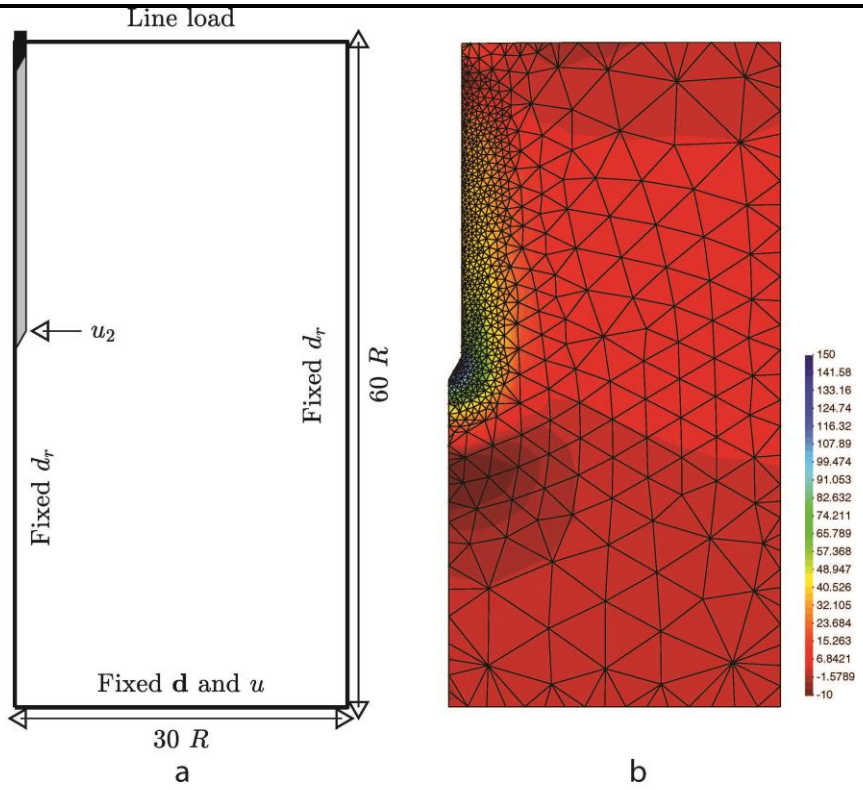

Figure 1

Accepted manuscript doi:
10.1680/jgele.18.00108

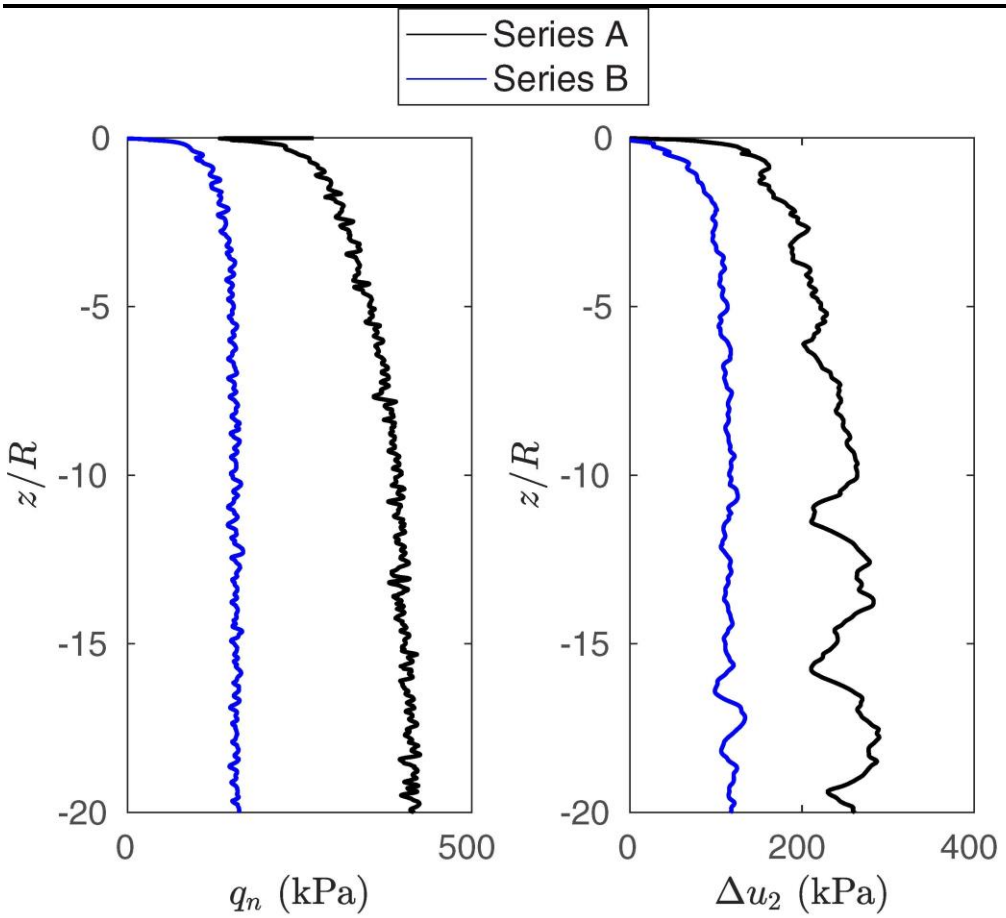

Figure 2

Accepted manuscript doi:
10.1680/jgele.18.00108

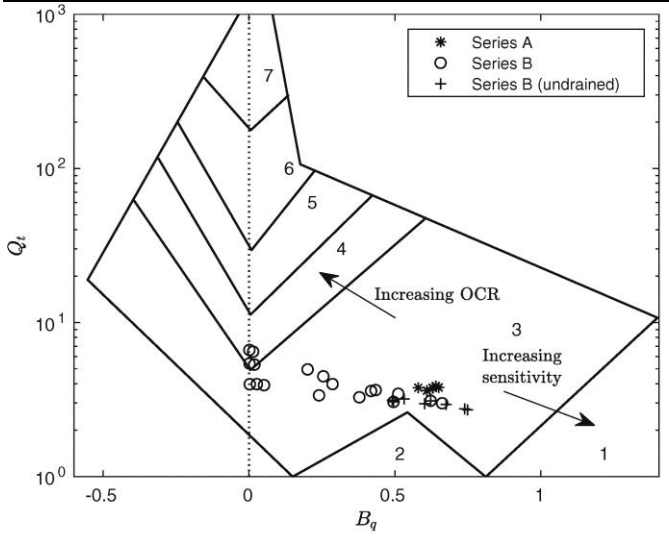

a

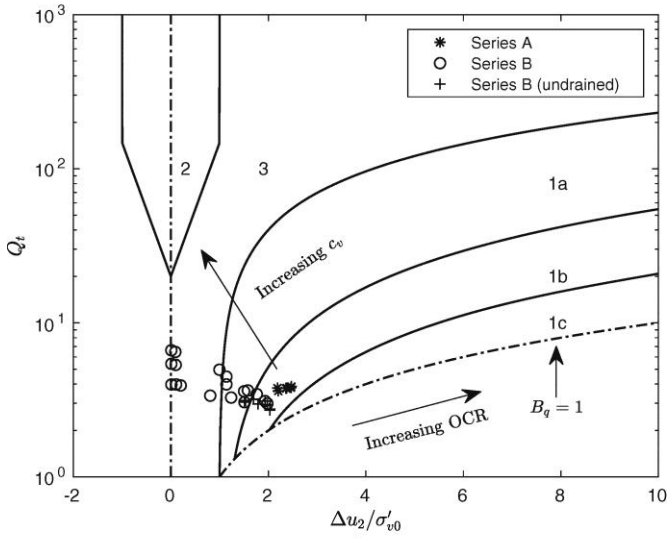

b

Figure 3

Accepted manuscript doi:
10.1680/jgele.18.00108

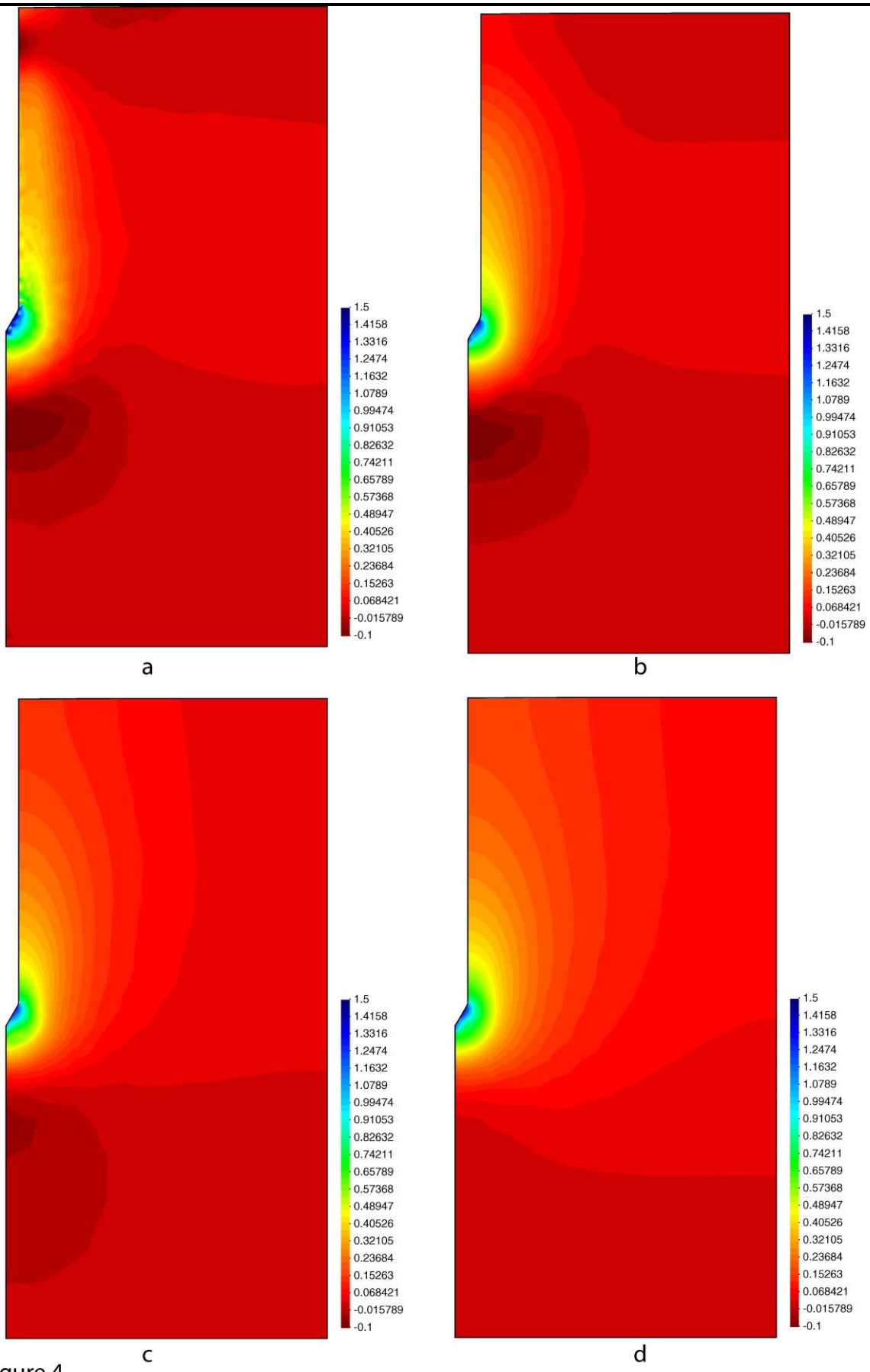

Figure 4

Accepted manuscript doi:
10.1680/jgele.18.00108

Accepted manuscript doi:
10.1680/jgele.18.00108

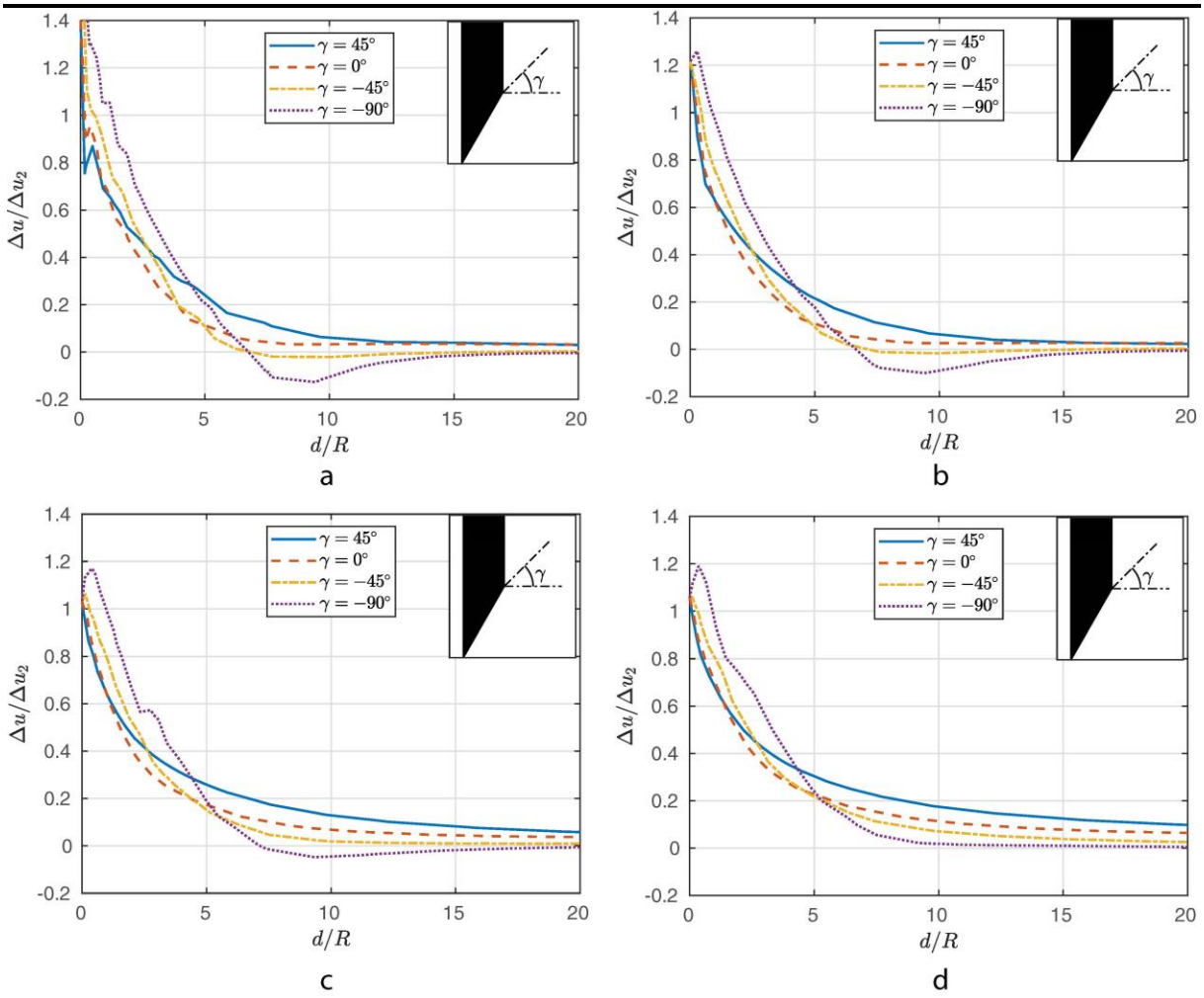

Figure 5

Accepted manuscript doi:
10.1680/jgele.18.00108

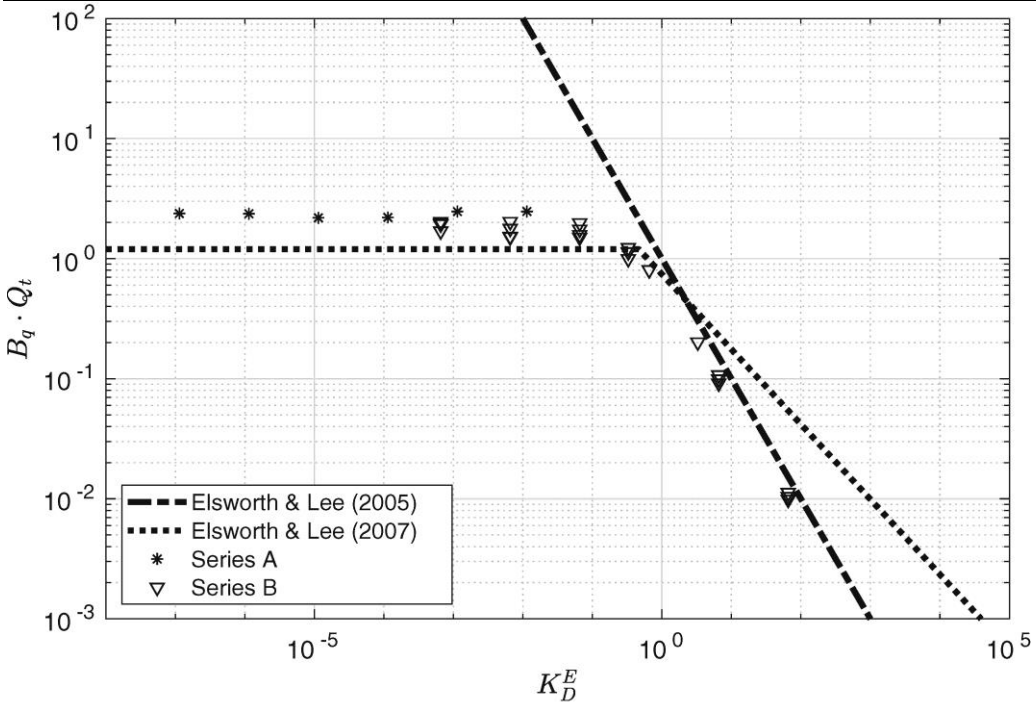

Figure 6

Accepted manuscript doi:
10.1680/jgele.18.00108

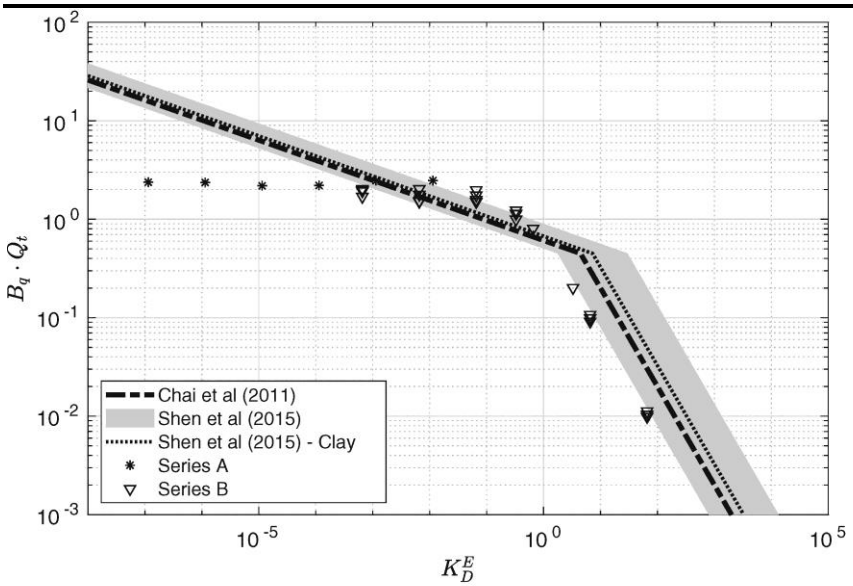

Figure 7

Accepted manuscript doi:
10.1680/jgele.18.00108

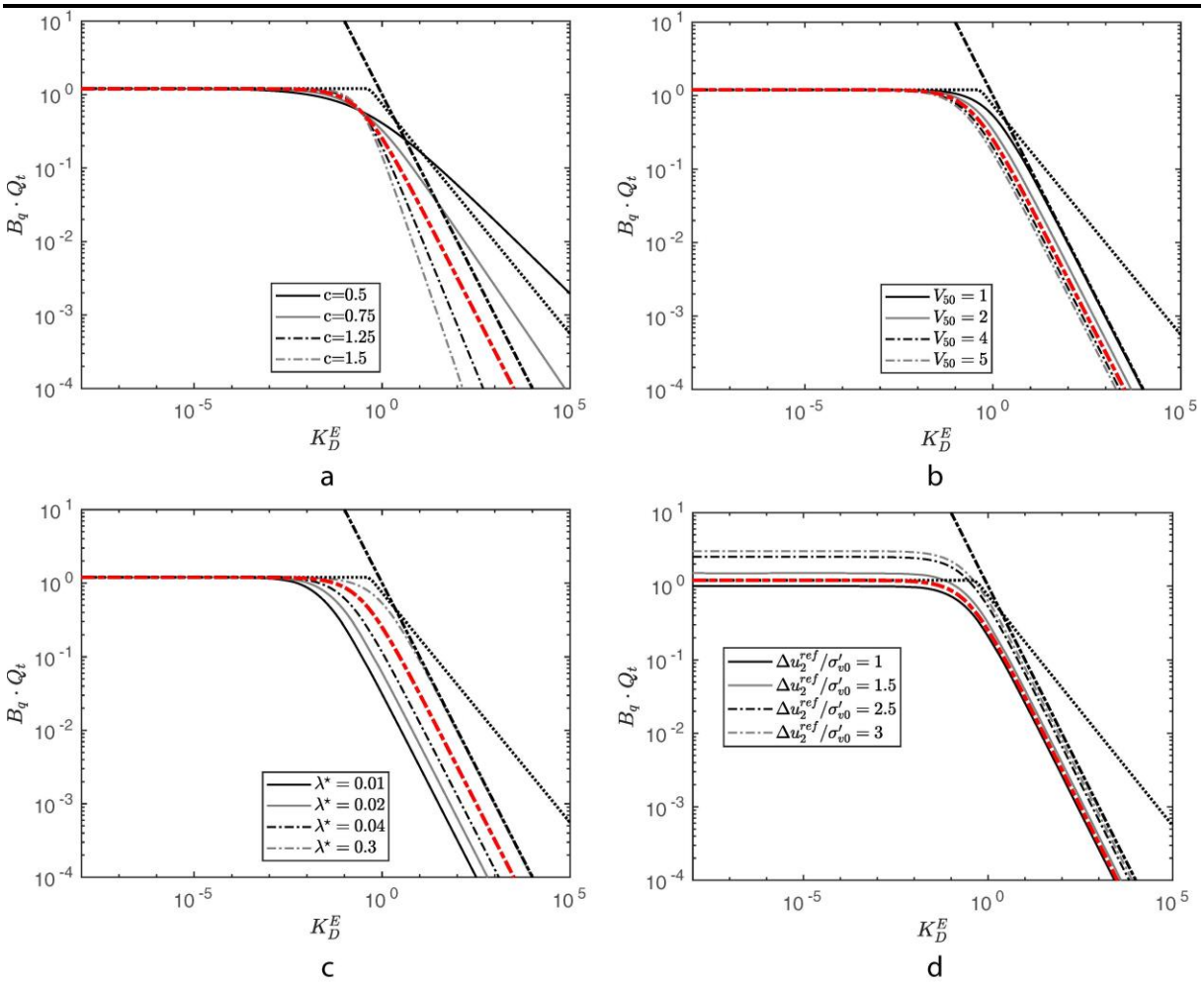

Figure 8

Accepted manuscript doi:
10.1680/jgele.18.00108

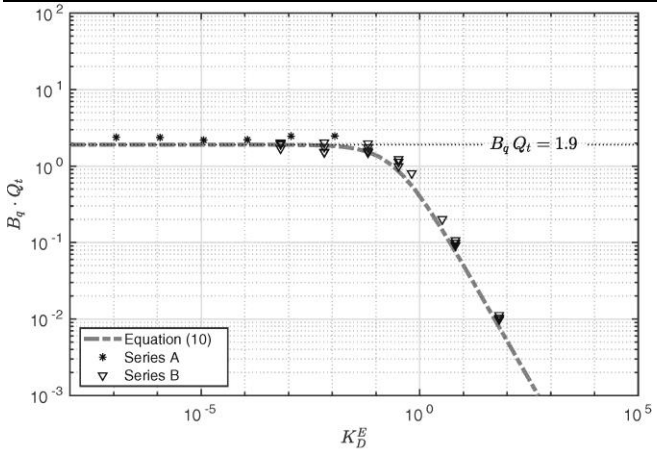

Figure 9

Accepted manuscript doi:
10.1680/jgele.18.00108

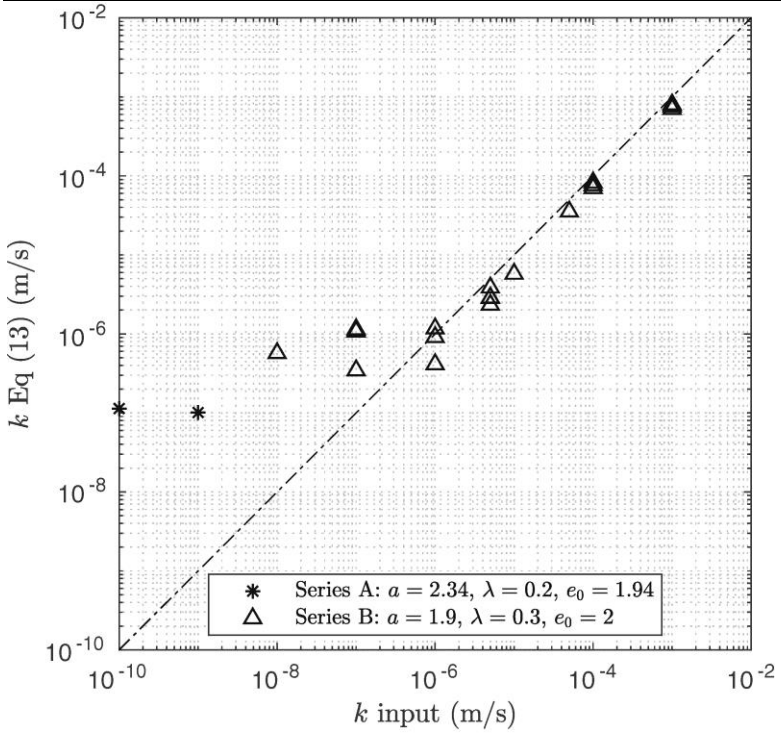

Figure 10

Accepted manuscript doi:
10.1680/jgele.18.00108

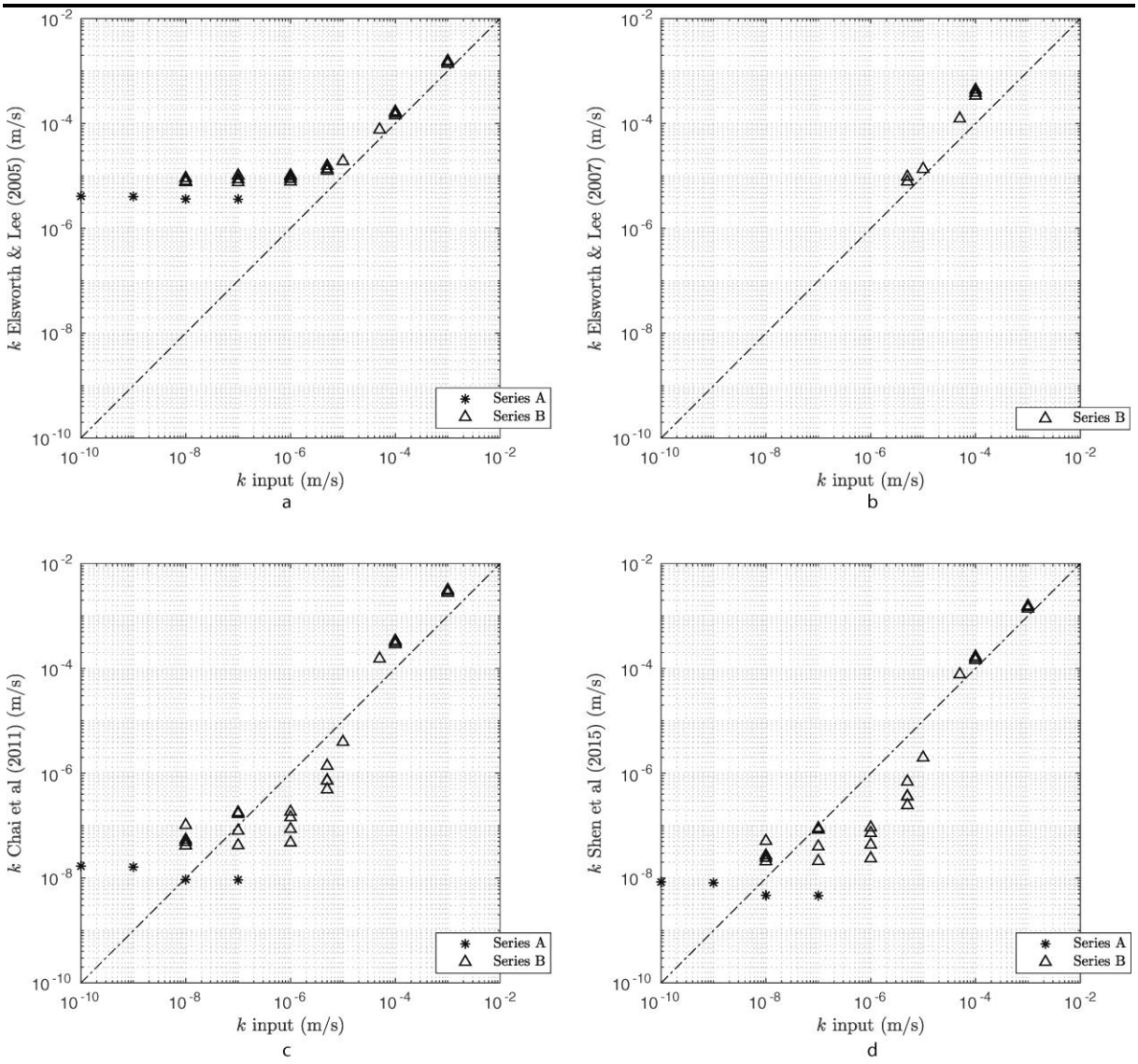

Figure 11